MULTISCIA
JOURNALS PUBLISHERS

FRONTIERS IN PHARMACEUTICAL ANALYSIS

ISSN: (3065- 1352)

https://multisciajournals.com/journals/index.php/fpa

editor.fpa1@gmail.com

Frontiers in Zoological Research
Volume 1 Issue 4 2025

Atlas of grass carp (Ctenopharyngodon idella) in single cells Peripheral blood IgM+ B cells shed light on teleost fish immunological responses mediated by B cells.

A Parimalagantham
Department of **Zoological Research**

Article Info

Received: 30-9-2025 Revised:08-11-2025 Accepted:19-11-2025 Published:29-11-2025

ABSTRACT

It is yet unknown how their immune systems react to bacterial infections. The transcriptome landscape of peripheral blood IgM+ B cells in grass carp (Ctenopharyngodon idella) was characterized in the current study using 10× Genomics single-cell RNA sequencing (scRNA-seq) after the fish were challenged with Aeromonas hydrophila, a significant aquatic pathogen. (im)mature B cells, innate B cells, proliferative B cells, IgDhigh B cells, and two infection-induced subsets known as infection Ⅰ and Ⅱ B cells are among the six transcriptionally different IgM+ B cell subpopulations that were found. Bacterial infection increased the immunological activation of circulating B cells, changed the cellular heterogeneity of IgM+ B cells, and caused metabolic reprogramming in (im)mature and innate B cell subpopulations. Interestingly, after being exposed to A. hydrophila, infection-induced B cells showed strong production of interferon φ1 (IFNφ1), a type I IFN. Teleost B cells actively contribute to innate antibacterial responses through IFN signaling, as demonstrated by the further validation of this induction through in vitro bacterial stimulation. Furthermore, peripheral blood persistently included the IgDhigh B cell subpopulation in both infected and uninfected conditions, suggesting a constitutive and probably mature phenotype. These discoveries greatly expand our knowledge of peripheral blood IgM+ B cell heterogeneity and offer fresh perspectives on IgM+ B cell-

teleost fish immunological responses that are mediated.

Keywords: Bacterial infection; B cells; peripheral blood; grass carp; ScRNA-seq

OVERVIEW

In animals, B cells travel from central lymphoid organs to peripheral immune sites via the circulatory system, where they develop and execute effector activities in response to immunological stimuli, including antibody generation and modulation of cellular immunity (Hoffman et al., 2016). The population of these cells is diverse and made up of different functional subsets (Bhattacharya, 2018). These subsets include memory B cells, regulatory B cells, plasma cells, and naïve B cells, all of which have different developmental histories (Akkaya et al., 2020; Lebien & Tedder, 2008; Shen & Fillatreau, 2015). Pathological circumstances, the local microenvironment, and aging all have an impact on the phenotypic and function of B cells (Cancro, 2020; Morgan & Tergaonkar, 2022). The B cell subpopulations of teleost fish, the first jawed vertebrates to display adaptive immune responses, are still poorly understood, especially in the

peripheral blood compartment, despite the fact that mammalian B cell subpopulations have been thoroughly described.

While five immunoglobulin isotypes (IgM, IgD, IgA, IgG, and Only three (IgM, IgD, and IgT) have been found in teleosts, although IgE has been described in mammals (Sun et al., 2020). Among them, all jawed vertebrates have the evolutionarily conserved isotype IgM (Amemiya et al., 2013). IgM+ B cells are the most prevalent type of B cells in teleosts and are essential for systemic immunity. Accepted on April 9, 2025; Received on March 8, 2025; Online on April 10, 2025 Zhang et al. (2010) responded. The immune cell landscape of a number of teleost species, such as the Mexican tetra (Astyanax mexicanus) (Ferrero et al., 2020; Peuß et al., 2020), zebrafish (Danio rerio) (Ferrero et al., 2020; Tang et al., 2017), rainbow trout (Oncorhynchus mykiss) (Perdiguero et al., 2021), grass carp (Ctenopharyngodon idella) (Pan et al., 2023), Nile tilapia (Oreochromis niloticus) (Wu et al., 2021), and Atlantic cod (Gadus morhua) (Guslund et al., 2020) have all had their immune cell landscapes thoroughly characterized thanks to recent advancements in single-cell RNA sequencing (scRNA-seq). MHC Ⅱ+ lymphocytes in rainbow trout's peripheral blood, which represent circulating B cells, have been categorized into ten clusters based on variations in routes of functional enrichment (Perdiguero et al., 2021). Six subpopulations of head kidney IgM+ B cells were identified by our earlier research in grass carp, including (im)mature B cells, innate B cells, growing B cells, plasma cells, CD22+ cells, and CD34+ cells (Pan et al., 2023). Furthermore, within primordially structured germinal center-like structures in the spleen of rainbow trout, clonal proliferation and somatic hypermutation of antigen (Ag)-specific IgM+ B cells have been seen (Shibasaki et al., 2023). Despite mounting evidence of teleost IgM+ B cell heterogeneity, little is known about their tissue-specific distribution and pathogen-responsive dynamics. Mammalian B cells carry out a variety of antibody-independent tasks in addition to their canonical involvement in antibody formation, chief among them being the release of immunomodulatory cytokines (Lund, 2008). B10 cells, which release interleukin-10 (IL-10) and inhibit CD4+ T cell responses, are one of the best-characterized cytokine-secreting subsets (Lykken et al., 2015). Be1 and Be2 cells are two types of effector B cells seen in mice; the former release IL-12, tumor necrosis factor-α (TNF-α), and interferon-γ (IFN-γ), while the latter release IL-4 and IL-10 (De Gruijter et al., 2022). B cells can also release cytokines in response to pathogen exposure; for example, parasite infection can increase B cell production of IL-17 (Hao et al., 2011), and bacterial and viral infection can produce CD11ahiFcγRIIIhi B cell subpopulations in mice that produce IFN-γ (Bao et al., 2014). Contrarily, cytokine-secreting B cells in teleosts are still little understood, despite growing interest in their distinctive intrinsic characteristics, like phagocytic activity. The existence of unidentified teleost B cell subpopulations, especially those that secrete cytokines, requires more research.

In this study, the pathogenic bacterium Aeromonas hydrophila was introduced to grass carp, and scRNA-seq was used to profile peripheral blood IgM+ B cells. Both infected and uninfected individuals consistently exhibited a unique IgDhigh B cell subpopulation, indicating a constitutive presence within the circulating IgM+ B cell compartment. Two subpopulations of infection-inducible IgM+ B cells were also discovered; one was characterized by increased CD9-like expression, while the other promoted innate immune responses by up-regulating IFNφ1. These results add to our knowledge of teleost B cell heterogeneity and offer fresh perspectives on the innate and adaptive characteristics of teleost fish B cell-mediated immunity.

SUPPLIES AND TECHNIQUES

Lead contact and the availability of materials

In this investigation, no novel reagents were

produced. Additionally

The lead contacts (Y.A.Z. and X.J.Z.) should be contacted for information and requests for resources and reagents, and they will handle these.

Statement of ethics

The Huazhong Agricultural University Animal Ethics Committee approved all animal experiments (HZAUFI-2024-0046), and every attempt was made to reduce animal suffering.

Bacterial infection and fish

We acquired healthy grass carp from Huanggang in Hubei Province, China, weighing roughly 150±20 g. At Huazhong Agricultural University's College of Fisheries, fish were kept in recirculating aquarium systems with regulated environmental conditions (27–29°C, 12-hour light/dark photoperiod). Before the trial, the fish were acclimated to the lab environment for at least two weeks and fed commercial meals twice a day. During this time, no clinical problems were noticed.

Our lab's A. hydrophila strain XS91-4-1 was utilized for the bacterial challenge.

The difficulty of bacteria

To achieve a final concentration of 7.5×106 CFU/mL, A. hydrophila was produced as previously described (Pan et al., 2023) and resuspended in sterile phosphate-buffered saline (PBS, Invitrogen, USA). Thirty grass carp were randomly assigned to two tanks (15 fish each), and 200 μL of either PBS (control) or A. hydrophila were injected intraperitoneally (i.p.).

Gathering tissue

Peripheral blood leukocytes were obtained from five fish per group sixteen days after infection. In short, fish were put to sleep using MS-222 (Sigma, USA), and heparinized needles were used to draw blood from the caudal vein. Dulbecco's Modified Eagle Medium (DMEM, Life Technologies, USA) supplemented with 100 U/mL penicillin, 100 μg/mL streptomycin, and 25 U/mL heparin (Sigma, USA) was used to dilute the samples ten times. As previously described (Zhang et al., 2010), leukocytes were separated by density gradient centrifugation using 51%/34% discontinuous Percoll (GE Healthcare, USA) and spun at 400 ×g for 30 minutes at 4°C. Leukocytes at the interface were gathered, resuspended in DMEM, rinsed twice with DMEM, and stored on ice until needed.

Sorting cells

The mouse anti-grass carp IgM monoclonal antibodies (1 μg/mL; 99-9-A4-A12) were treated with leukocytes for 45 minutes on ice in PBS that included 2% fetal bovine serum (FBS, Thermo Fisher Scientific, USA) (Cui et al., 2020). Following three washes, cells were resuspended in PBS with 2% FBS (Gibco, New Zealand) and treated for 30 minutes on ice with allophycocyanin-conjugated goat anti-mouse IgG antibodies (2 μg/mL; BioLegend, USA). Cells were resuspended in PBS containing 5 μg/mL propidium iodide (PI; Thermo Fisher Scientific, USA) for 5 minutes after three more washes. Fluorescence-activated cell sorting (FACS) using MoFlo XDP (Beckman, USA) was used to isolate live IgM-positive cells. Using the forward-scatter (FSC)/side-scatter (SSC) profile and PI fluorescence, the gating technique was used to remove dead cells, adherent cells, and cell debris from the sorted IgM+ B cells.

Sequencing and preparation of single-cell libraries

Sorted IgM+ B cell single-cell transcriptome libraries

In response, Zhang et al. (2010). Recent advances in single-cell RNA sequencing (scRNA-seq) have allowed for a thorough characterization of the immune cell landscapes of several teleost species, including the Nile tilapia (Oreochromis niloticus) (Wu et al., 2021), the Atlantic cod (Gadus morhua) (Guslund et al., 2020), rainbow trout (Oncorhynchus mykiss) (Perdiguero et al., 2021), grass carp (Ctenopharyngodon idella) (Pan et al., 2023), and the Mexican tetra (Astyanax mexicanus) (Ferrero et al., 2020; Peuß et al., 2020). Ten clusters of MHC₡+ lymphocytes, which are indicative of circulating B cells, have been identified in the peripheral blood of rainbow trouts based on

Regarding differences in functional enrichment pathways (Perdiguero et al., 2021). In grass carp, we previously found six subpopulations of head kidney IgM+ B cells: (im)mature B cells, innate B cells, expanding B cells, plasma cells, CD22+ cells, and CD34+ cells (Pan et al., 2023). Additionally, clonal proliferation and somatic hypermutation of antigen (Ag)-specific IgM+ B cells have been observed within primordially formed germinal center-like structures in the rainbow trout spleen (Shibasaki et al., 2023). Although teleost IgM+ B cell heterogeneity is becoming more and more evident, little is understood regarding their pathogen-responsive dynamics and tissue-specific distribution. In addition to their classical role in antibody generation, mammalian B cells perform a number of antibody-independent functions, the most important of which is the release of immunomodulatory cytokines (Lund, 2008). One of the most well-studied cytokine-secreting subsets is B10 cells, which suppress CD4+ T cell responses and release interleukin-10 (IL-10) (Lykken et al., 2015). Two types of effector B cells, known as Be1 and Be2, are seen in mice; the former produce IL-12, interferon-γ (IFN-γ), and tumor necrosis factor-α (TNF-α), while the latter release IL-4 and IL-10 (De Gruijter et al., 2022). In response to pathogen exposure, B cells can also release cytokines. For instance, parasite infection can boost B cell production of IL-17 (Hao et al., 2011), and bacterial and viral infection can result in CD11ahiFcγRIIIhi B cell subpopulations in mice that produce IFN-γ (Bao et al., 2014). On the other hand, despite increased interest in their unique intrinsic traits, such as phagocytic activity, little is known about cytokine-secreting B cells in teleosts. Further investigation is needed into the existence of unidentified teleost B cell subpopulations, particularly those that release cytokines.

In this study, grass carp were exposed to the pathogenic bacterium Aeromonas hydrophila, and peripheral blood IgM+ B cells were profiled using scRNA-seq. A distinct IgDhigh B cell subpopulation was consistently seen in both infected and uninfected individuals, suggesting a constitutive presence within the circulating IgM+ B cell pool. We also identified two subpopulations of infection-inducible IgM+ B cells, one of which exhibited elevated CD9-like expression and the other of which up-regulated IFNφ1 to stimulate innate immune responses. These findings broaden our understanding of the diversity of teleost B cells and provide new insights into the innate and adaptive features of B cell-mediated immunity in teleost fish.

TECHNIQUES AND SUPPLIES

Lead communication and material accessibility

No new reagents were created for this study. Furthermore,

Requests for resources and reagents, as well as information, should be directed to the lead contacts, Y.A.Z. and X.J.Z.

Ethics statement

Every effort was made to minimize animal suffering, and all animal studies were authorized by the Huazhong Agricultural University Animal Ethics Committee (HZAUFI-2024-0046).

Fish and bacterial infections

We purchased healthy grass carp weighing about 150±20 g from Huanggang in Hubei Province, China. Fish were housed in recirculating tank systems with controlled climatic conditions (27–29°C, 12-hour light/dark photoperiod) at the College of Fisheries at Huazhong Agricultural

University. The fish were given commercial meals twice a day and allowed to get used to the lab environment for at least two weeks prior to the trial. No clinical issues were observed over this period.

The strain of A. hydrophila XS91-4-1 from our lab was used for the bacterial challenge. The challenge posed by microbes A. hydrophila was prepared as previously reported (Pan et al., 2023) and resuspended in sterile phosphate-buffered saline (PBS, Invitrogen, USA) to reach a final concentration of 7.5×106 CFU/mL. Thirty grass carp were divided into two tanks (15 fish each) at random, and 200 μL of either A. hydrophila or PBS (control) were injected intraperitoneally (i.p.). Collecting tissues Sixteen days following infection, five fish per group had their peripheral blood leukocytes extracted. To put it briefly, fish were put to sleep using MS-222 (Sigma, USA), and blood was extracted from the caudal vein using heparinized needles. The samples were diluted ten times using Dulbecco's Modified Eagle Medium (DMEM, Life Technologies, USA) supplemented with 100 U/mL penicillin, 100 μg/mL streptomycin, and 25 U/mL heparin (Sigma, USA). Leukocytes were isolated by density gradient centrifugation using 51%/34% discontinuous Percoll (GE Healthcare, USA) and spun at 400 ×g for 30 minutes at 4°C, as previously reported (Zhang et al., 2010). DMEM was used to resuspend leukocytes at the interface, clean them twice, and then store them on ice until they were needed.

Cell sorting

For 45 minutes on ice in PBS containing 2% fetal bovine serum (FBS, Thermo Fisher Scientific, USA), leukocytes were used to treat the mouse anti-grass carp IgM monoclonal antibodies (1 μg/mL; 99-9-A4-A12) (Cui et al., 2020). After three washes, cells were resuspended in PBS containing 2% FBS (Gibco, New Zealand) and exposed to allophycocyanin-conjugated goat anti-mouse IgG antibodies (2 μg/mL; BioLegend, USA) for 30 minutes on ice. After three further washes, cells were resuspended in PBS with 5 μg/mL propidium iodide (PI; Thermo Fisher Scientific, USA) for five minutes. Live IgM-positive cells were isolated by fluorescence-activated cell sorting (FACS) using MoFlo XDP (Beckman, USA). Dead cells, adherent cells, and cell debris were eliminated from the sorted IgM+ B cells using the gating technique, which was based on the forward-scatter (FSC)/side-scatter (SSC) profile and PI fluorescence.

Single-cell library preparation and sequencing

Sorted single-cell transcriptome libraries of IgM+ B cells PBS as a control or A. hydrophila (cell:bacterium=1:10). The length of time that the cells were incubated at 28°C varied based on the experimental setup.

Polymerase chain reaction (qPCR) of excited cells in real time

As directed by the manufacturer, total RNA was extracted from stimulated IgM+ B cells using a HiPure Total RNA Plus Mini Kit (R4121; Magen, China). As directed by the manufacturer, reverse transcription was carried out using a PrimeScript™ FAST RT reagent Kit with gDNA Eraser (RR092S; Takara, Japan). The CFX96 Connect Real-time System (BioRad, USA) with ChamQ SYBR Color qPCR Master Mix (Q411-02; Vazyme, China) was used to measure the transcript levels of IFNφ1 and associated pathway genes. TLR3-F, 5' GAG AAC AAT CGT GAC TCC CTG A 3'; TLR3-R, 5' CCA GTA; IFNφ1-F, 5' AAG CAA CGA GTC TTT GAG CCT 3'; IFNφ1-R, 5' GCG TCC TGG AAA TGA CAC CT 3'; and β-actin-F, 5' AGC CAT CCT TCT TGG GTA TG 3'; β-actin-R, 5' GGT GGG GCG ATG ATC TTG AT 3' TLR7-F, 5' GAG CAT ACA GTT GAG TAA ACG CAC 3'; TLR7-R, 5' TCT CCA AGA ATA TCA GGA CGA TAA 3'; TLR8-F, 5' TCA CAT CGC TTC CAG GTC TC 3'; TLR8-R, 5' ACG GTG AAA

TAA TGG GGG TT 3'. Using the 2−△△CT technique, relative expression levels were determined.

Analysis of statistics

Using GraphPad Prism (v.7.0), one-way analysis of variance (ANOVA) with Dunnett's post hoc test was used to examine variations in the expression levels of IFNφ1 and IFN-related pathway molecules. The mean±standard deviation (SD) is used to display the data. Using

the Wilcoxon test and the "stat_compare_means" function in the "ggpubr" package (v.0.6.0), additional statistical analyses were carried out in R.

OUTCOMES

Different peripheral blood IgM+ B cell subpopulations are identified by ScRNA-seq under various circumstances.
The 10× Genomics platform was used to perform scRNA-seq in order to fully capture the molecular repertoire of grass carp peripheral blood IgM+ B cells at single-cell resolution (Figure 1A; Supplementary Figure S1). Six different lineages were identified from the analysis and visualization of 31,959 high-quality cells using Uniform Manifold Approximation and Projection (UMAP): (im)mature B cells, innate B cells, IgDhigh B cells, proliferating B cells, infection I B cells, and infection II B cells (Figure 1B; Supplementary Table S1). Established marker genes were used to identify innate and proliferating B cells: Ki-67, UBE2C, TOP2a, and AID for proliferating B cells, and IRF8, CCL4, and IRF4b for innate B cells (Hu et al., 2024; Pan et al., 2023) (Figure 1C). According to Lopez-Medina et al. (2015), a new subpopulation known as IgDhigh B cells (Figure 1C, D) was discovered that expressed high quantities of Igδs and PD-L1. The percentage of IgDhigh B cells rose from 4.15% to 6.66% after the bacterial challenge (Figure 1E). Notably, following infection, two new subpopulations—infection I and II B cells—emerged. Increased expression of MHCIIα, IFI27L2a, GIG2i, ISG152, Mx3, and STAT1 (Bénard et al., 2018; Wirz et al., 2022) was seen in infection I B cells (Figure 1C, D), whereas infection II B cells mostly expressed CD9-like (Figure 1C, D) (Castro

(2015) et al.
Functional description of peripheral blood IgM+ B cell subpopulations that have been conserved
Because they were seen in both control and infected grass carp, the (im)mature, innate, proliferating, and IgDhigh B cells were classified as conserved subpopulations. Of them, TNF-α, Myc-2, and CD37 expression were up-regulated in IgDhigh and growing B cells (Pearson et al., 2001; Van Spriel et al., 2012) (Figure 2A). Furthermore, these B cells also included CD68, which is often regarded as a macrophage marker (Figure 2A). This discovery supports the theory that ancient phagocytes may have given rise to vertebrate B cells. According to earlier research, a subset of B cells in zebrafish is identified by macrophage-expressed gene 1 (mpeg) (Ferrero et al., 2020; Han et al., 2024), indicating a common ancestry between B cells and macrophages in early vertebrates. CD300a and CAPG, genes associated with migratory potential and innate function (Dabiri et al., 1992; Silva et al., 2011), were expressed more often in innate B cells (Figure 2A). According to studies by Baik et al. (2007), Repasky et al. (2004), and Takase et al. (1995), proliferating B cells have high levels of PCNA, STMN1, TPX2, and DNTTIP1, which is consistent with active cell cycle progression and the possibility of clonal expansion and VDJ rearrangement (Figure 2A). Proliferating B cells were shown to be enriched in pathways associated with "Cell division," "Cell cycle," "Regulation of mitotic cell cycle phase transition," and "DNA replication," according to GO enrichment analysis (Figure 2B). IgDhigh B cells, on the other hand, were enriched in pathways associated with "translation," "phagocytosis," "innate immune response activation," and "peptide biosynthesis" (Figure 2B). Igμ2 was the most highly expressed gene, according to an analysis of IgM heavy chain gene expression (Figure 2C). Proliferating B cells had the highest Igμs expression among the subpopulations, followed by IgDhigh B cells, innate B cells, and (im)mature B cells (Figure 2C). Expression patterns of genes linked to B cell differentiation were examined in order to evaluate the developmental maturity of the B cell subpopulations (Zwollo, 2011). Blimp1 was not expressed by proliferating B cells, although PAX5 and XBP1 were highly expressed. Blimp1, IRF4a, and XBP1 were all expressed more in innate B cells than in IgDhigh B cells (Figure 2D).
alterations in conserved IgM+ B cell metabolic

patterns after bacterial infection In steady-state settings, metabolic activity was assessed across conserved IgM+ B cell subpopulations. OXPHOS, ETC, fatty acid metabolism, glycolysis, pentose phosphate shunt, and TCA were among the important metabolic pathways evaluated. The findings showed that innate B cells and IgDhigh had higher aging ratings than (im)mature and proliferating B cells (Figure 3A), while apoptosis scores were almost the same for all subpopulations. The highest levels of OXPHOS and ETC activity were seen in proliferating B cells, which is probably due to their higher energy requirements for cell cycle progression (Figure 3A). Interestingly, IgDhigh B cells used fatty acid metabolism instead of glycolysis to provide energy (Figure 3B). The pentose phosphate shunt score was significantly higher in proliferating B cells, indicating improved nucleotide biosynthesis and redox control, although no discernible changes in fatty acid metabolism or glycolysis were seen between proliferating and (im)mature B cells (Figure 3B).

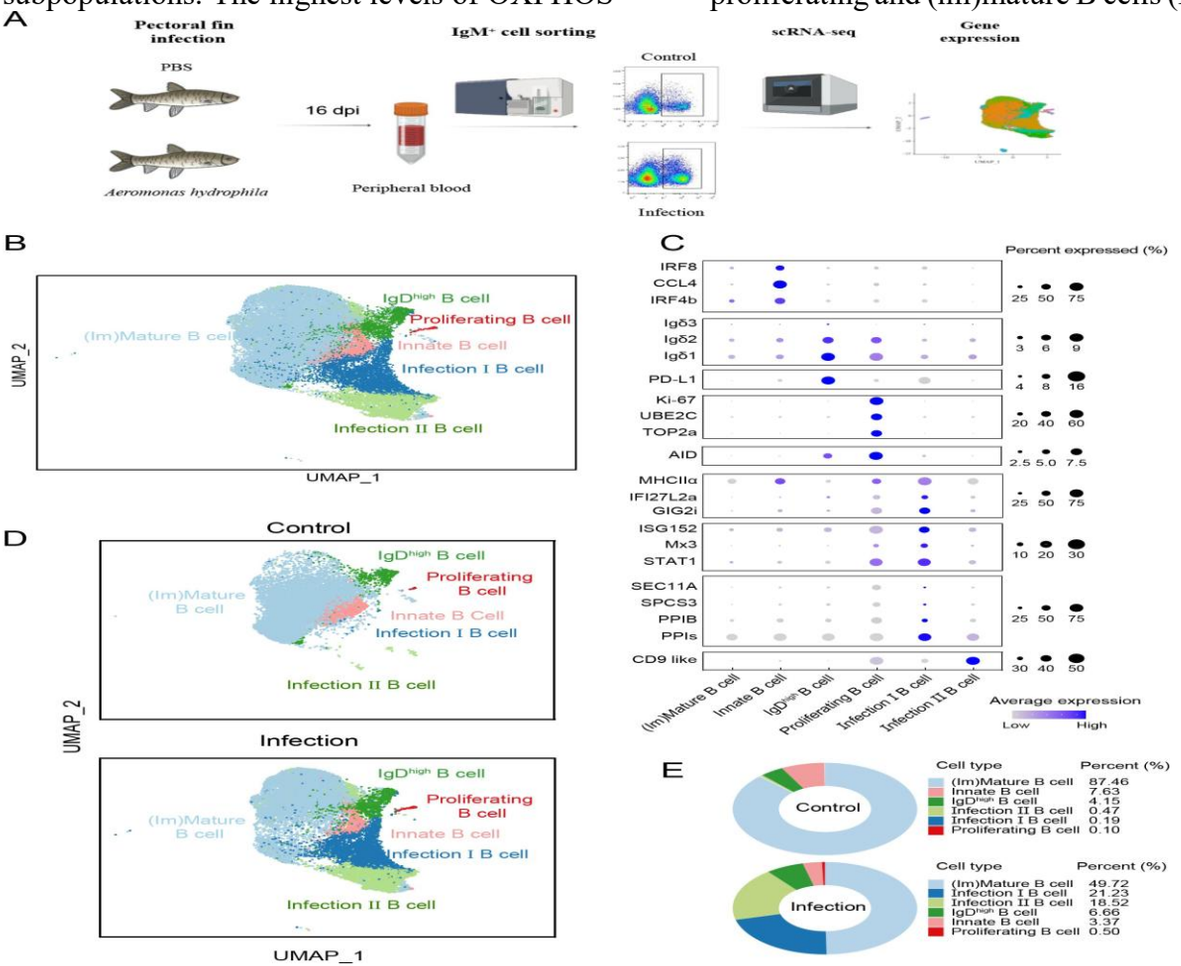

Figure 1 Characterization of grass carp IgM⁺ B cells in peripheral blood

A: Schematic representation of experimental workflow, including bacterial infection, cell sorting, and scRNA-seq analysis. B: UMAP visualization of 31 959 peripheral blood IgM⁺ B cells from control (12 034 cells) and infected (19 925 cells) grass carp. Each dot represents a single cell, colored according to cell subpopulation. C: Dot plots depicting expression of selected marker genes in peripheral blood IgM⁺ B cell subpopulations. D: UMAP visualization of peripheral blood IgM⁺ B cells from control or infected grass carp. Each dot represents a single cell, colored according to cell subpopulation. E: Proportional representation of each IgM⁺ B cell subpopulation in control and infected grass carp.

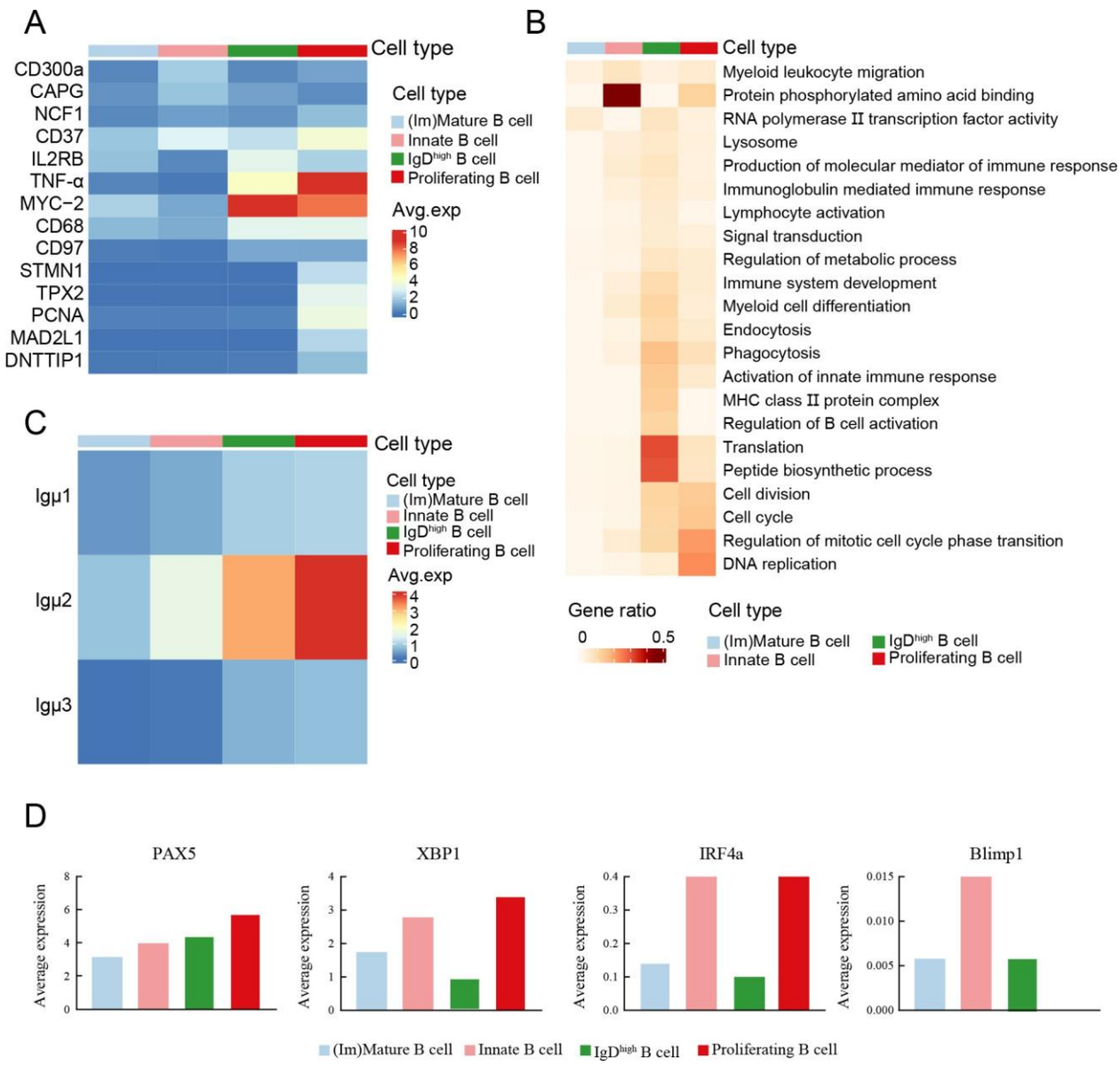

Figure 2 Characterization of IgM⁺ B cell subpopulations in control grass carp

A: Heatmap displaying expression of DEGs in conserved B cell subpopulations. GenBank accession numbers are as follows: CMRF35-like molecule 8 (*CD300a*: XM_051886229.1), macrophage-capping (*CAPG*: XM_051893361.1), neutrophil cytosolic factor 1 (*NCF1*: KX243421.1), cluster of differentiation 37 (*CD37*: XM_051914834.1), interleukin-2 receptor subunit beta (*IL2RB*: XM_051895906.1), tumor necrosis factor-alpha (*TNF-α*: JQ040498.1), transcriptional regulator Myc-2 (*Myc-2*: XM_051897435.1), cluster of differentiation 68 (*CD68*: XM_051898922.1), cluster of differentiation 97 (*CD97*: XM_051885655.1), stathmin (*STMN1*: PQ678985), targeting protein for Xklp2-B (*TPX2*: XM_051880612.1), proliferating cell nuclear antigen (*PCNA*: PQ678986), mitotic spindle assembly checkpoint protein MAD2A like (*MAD2AL1*: XM_051899820.1), deoxynucleotidyl transferase terminal-interacting protein 1 (*DNTTIP1*: XM_051897763.1). Avg.exp represents normalized average expression value of a gene within cell subpopulations. B: Gene Ontology (GO) analysis of DEGs for each

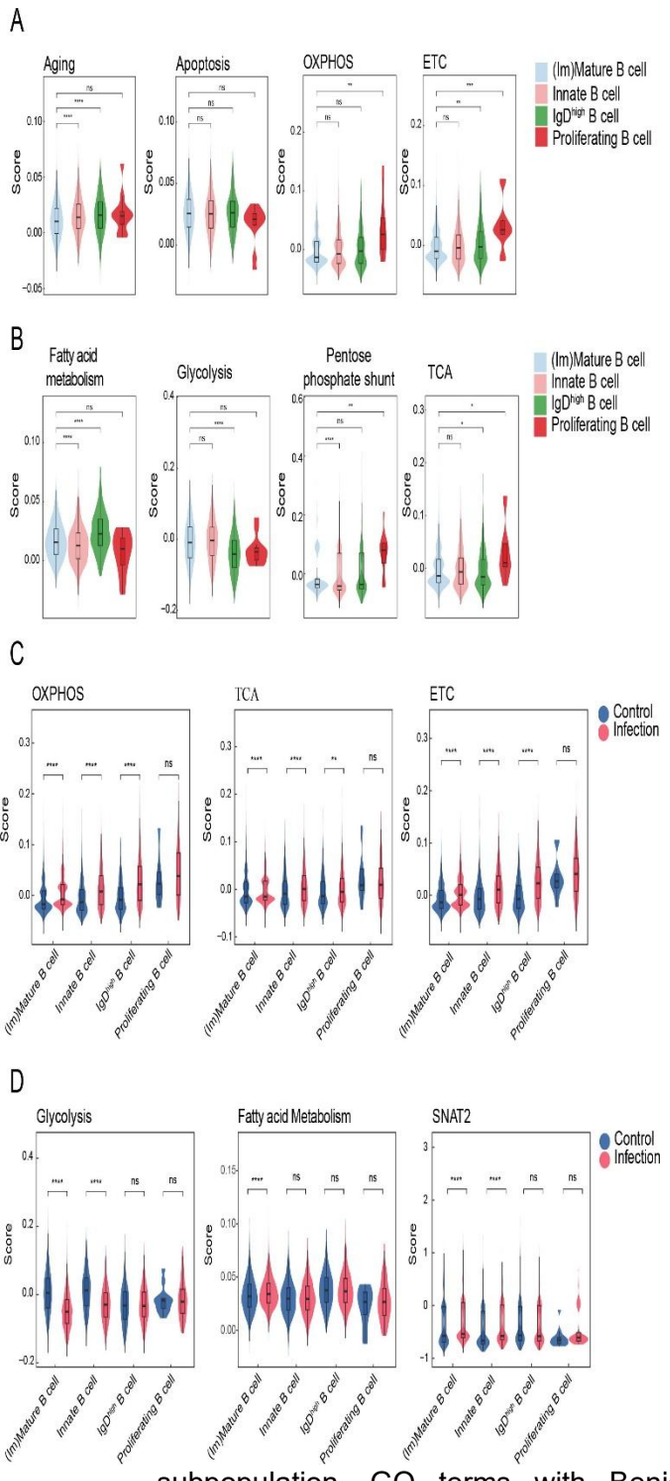

subpopulation. GO terms with Benjamini-Hochberg-corrected *P*-values<0.05 (one-sided Fisher's exact test) were selected and colored by gene ratio. C: Heatmap illustrating average expression of each *Igμ* subtype in conserved B cell subpopulations. Avg.exp represents normalized average expression value of a gene within cell subpopulations. D: Bar chart showing average expression of B cell differentiation-related genes in conserved B cell subpopulations. GenBank accession numbers of genes are as follows: paired box 5 (*PAX5*: XM_051888673.1), X-box binding protein 1 (*XBP1*: XM_051894190.1), interferon regulatory factor 4a (*IRF4a*: KU182644.1), B lymphocyte induced maturation protein 1 (*Blimp1*: XM_051866097.1).

Bacterial infection can alter the metabolic state of immune cells (Bantug et al., 2018). Except for proliferating B cells, which maintained stable profiles, the remaining conserved subpopulations showed significant up-regulation of OXPHOS, TCA, and ETC activity following bacterial infection (Figure 3C). Fatty acid metabolism was specifically increased in (im)matureB cells (Figure 3D), while glycolytic activity declined in both (im)mature and innate B cells. Concurrently, the expression of sodium-dependent neutral amino acid transporter-2 (*SNAT2*) was significantly increased, suggesting that glutamine metabolism may play a key role in these two B cell subpopulations following infection (Zwollo, 2011) (Figure 3D).

Figure 3 Metabolic process of conserved IgM⁺ B cell subpopulations

A: Violin plots showing aging, apoptosis, oxidative phosphorylation (OXPHOS), and electron transport chain (ETC) scores for each conserved IgM⁺ B cell subpopulation. B: Violin plots depicting fatty acid metabolism, glycolysis, pentose phosphate shunt, and tricarboxylic acid (TCA) cycle scores for each conserved IgM⁺ B cell subpopulation. C: Comparison of OXPHOS, TCA, and ETC scores for each conserved IgM⁺ B cell subpopulation from control and infected grass carp

Differentiation states of conserved IgM⁺ B cells following bacterial infection

Bacterial infection did not induce the transcription of immunoglobulin genes in any conserved IgM⁺ B cell subpopulation (Figure 4A). However, *PAX5* expression was uniformly up-regulated, while *XBP1* and *IRF4a* were down- regulated across all subsets following infection (Figure 4B). The expression levels of *TXNIP*, *SESN1*, *JunB*, and *GADD45B* (Frasca et al., 2019; García-Vega et al., 2024; Shao et al., 2010) as well as *KLF2*, *FOXO3*, *MCL1*, and *CD79b* (Hart et al., 2011; Hinman et al., 2009; Opferman et al., 2003), were up-regulated in all conserved subpopulations upon bacterial infection (Figure 4C). In contrast, the expression levels of *MHCⅡα* and *MHCⅡβ* were down-regulated (Figure 4C). Although phagocytic capacity was improved in (im)mature, IgD^{high}, and innate B cells following bacterial infection, their antigen processing and presentation capabilities were weakened (Figure 4D). To further characterize infection-induced differentiation dynamics, pseudotime trajectories were reconstructed using Monocle, alongside RNA velocity analysis. Result demonstrated a shift in the developmental trajectories of IgM⁺ B cell subpopulations following infection (Figure 4E). RNA velocity analysis revealed a lack of clear polarized differentiation directions, consistent with Monocle predictions; however, all trajectories converged toward the infection Ⅰ B cell state, indicating a unified transcriptional response to bacterial challenge (Figure 4F).

Characterization of infection-induced IgM⁺ B cell subpopulations

Infection Ⅰ and Ⅱ B cells, which emerged following infection with *A. hydrophila*, exhibited a greater number of detected genes compared to (im)mature B cells, indicating higher transcriptional activity (Figure 5A). Based on their transcriptional signatures (Figure 1B), infection Ⅰ B cells were defined by robust expression of *IFNφ1*, a gene classically associated with antiviral responses but also implicated in antibacterial defense (Xiao et al., 2021; Zhu et al., 2023). As Toll-like receptors are key sensors of pathogen-associated molecular patterns (e.g., lipopolysaccharides) and are essential for initiating inflammatory responses (Su, 2025), the expression of TLRs and related signaling components was examined. Infection Ⅰ B cells displayed coordinated up-regulation of IFN signaling genes such as *TLRs*, *cGAS*, and *STING* (Erttmann et al., 2022) (Figure 5B). Stimulation of peripheral blood IgM⁺ B cells with heat-inactivated *A. hydrophila* for 4, 12, and 24 h resulted in significant up- regulation of *IFNφ1* and associated IFN pathway genes (Figure 5C), consistent with the scRNA-seq results. To assess whether these newly emerged subpopulations possess distinct antibody-secreting capacities, the expression of *Igμs* was quantified post-infection. Results showed that *Igμs* expression in the newly emerged subpopulations was similar to that in (im)mature B cells, suggesting that these cells are not differentiating toward plasma cells (Figure 5D). Pseudotime trajectory analysis revealed that both infection I and II B cells predominantly occupied terminal positions along the differentiation axis (Figure 5E).

KEGG pathway enrichment analysis showed that infection Ⅰ B cells were significantly enriched in pattern recognition receptor-related pathways, including “Toll-like receptor signaling pathway”, “RIG-I-like receptor signaling pathway”, “NOD-like receptor signaling pathway”, and “C-type lectin

receptor signaling pathway" (Figure 5F), while infection Ⅱ B cells were enriched in "FC gamma R-mediated phagocytosis"
and "FoxO signaling pathway" (Figure 5F). Detailed pathway identifiers, expression levels, and statistical significance are provided in Supplementary Table S2.

Co-expression of immunoglobulin genes in peripheral blood IgM⁺ B cells

The subtypes of grass carp IgM (*Igμ*) and IgD (*Igδ*) heavy chain genes have been described in our previous study (Pan et al., 2023). Here, co-expression patterns of *Igμs* and *Igδs* were examined at the single-cell level in peripheral blood IgM⁺ B cells from both control and infected grass carp. Among the *Igμ* transcripts, the most frequently observed pattern was *Igμ1⁻Igμ2⁺Igμ3⁻*, followed by *Igμ1⁺Igμ2⁻Igμ3⁻* and *Igμ1⁺Igμ2⁺Igμ3⁻* (Figure 6A). Following bacterial infection, the percentage of IgM⁺ B cells co-expressing *Igμs* increased, with enriched patterns such as *Igμ1⁺Igμ2⁺Igμ3⁻*, *Igμ1⁺Igμ2⁻Igμ3⁺*, *Igμ1⁻Igμ2⁺Igμ3⁺*, and *Igμ1⁺Igμ2⁺Igμ3⁺*. Co-expression patterns of *Igδs* isoforms were also analyzed. The most common expression pattern in IgM⁺ B cells was *Igδ1⁺Igδ2⁻Igδ3⁻*, followed by *Igδ1⁻Igδ2⁺Igδ3⁻* (Figure 6B). Notably, in contrast to *Igμs*, co-expression of *Igδs* variants was very low and unaffected by bacterial infection (Figure 6B).

Further analysis of co-expression profiles across individual B cell subpopulations revealed no major infection-induced changes in *Igμs* and *Igδs* co-expression patterns, with the exception of proliferating and IgD^{high} B cells. In the control group, the highest co-expression rate of *Igμs* and *Igδs* in proliferating B cells was 8.33%, with dominant patterns including *Igμ1⁻Igμ2⁺Igμ3⁻Igδ1⁻Igδ2⁺Igδ3⁻*, *Igμ1⁺Igμ2⁺Igμ3⁺ Igδ1⁺Igδ2⁻Igδ3⁻*, and *Igμ1⁺Igμ2⁺Igμ3⁺Igδ1⁺Igδ2⁺Igδ3⁻* (Figure 6C). Post-infection, this co-expression rate declined to 3.03%, with prevalent configurations such as *Igμ1⁻Igμ2⁺ Igμ3⁻Igδ1⁺Igδ2⁻Igδ3⁻*, *Igμ1⁻Igμ2⁺Igμ3⁻Igδ1⁻Igδ2⁺Igδ3⁻*, and *Igμ1⁺Igμ2⁺Igμ3⁺Igδ1⁺Igδ2⁻Igδ3⁻* (Figure 6D). A similar reduction in the co-expression rate was observed in IgD^{high} B cells, decreasing from 26.80% to 12.80% after infection (Figure 6C, D).

DISCUSSION

Our earlier work in rainbow trout revealed that B cells represent a substantial fraction of peripheral blood lymphocytes in teleosts, accounting for approximately 57% of circulating lymphocytes (Zhang et al., 2010). This high prevalence underscores the importance of elucidating the heterogeneity of peripheral B cells in these early vertebrates to improve our understanding of immunological roles during homeostasis and infection.

In mammals, peripheral B cells are well recognized as a phenotypically diverse population, exhibiting distinct differentiation and functional states, including IgD⁺CD27⁻ naïve B cells, IgD⁻CD27⁺ memory B cells, and IgD⁻CD27^{high} plasmablasts (Kaminski et al., 2012; Meeuwsen et al., 2017; Sanz et al., 2008). While long-lived plasma cells preferentially localize to the bone marrow, memory B cells exhibit tissue- specific distribution and context-dependent expression signatures (Chen & Laidlaw, 2022; Fooksman et al., 2024). However, comparable insight into the tissue-specific heterogeneity of B cells in teleosts remains limited. Our previous single-cell transcriptomic analysis of grass carp head kidney identified six major IgM⁺ B cell subpopulations: (im)mature B cells, innate B cells, proliferating B cells, plasma

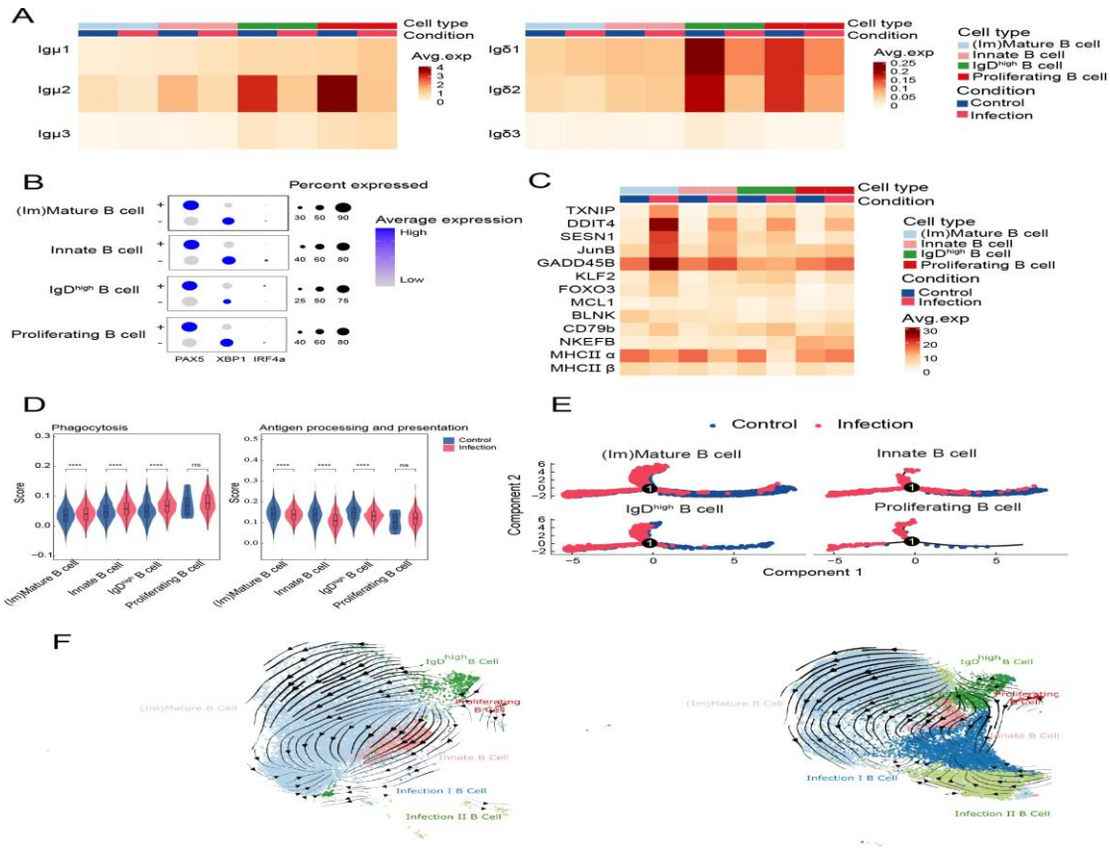

Figure 4 Effects of infection on conserved peripheral blood IgM⁺ B cells

A: Heatmap showing average expression of each *Igμ* (left) and *Igδ* (right) subtype in each conserved IgM⁺ B cell subpopulation. Avg.exp represents normalized average expression value of a gene within cell subpopulations. B: Dot plot showing expression of B cell differentiation-related genes in each conserved IgM⁺ B cell subpopulation before (-) and after (+) *A. hydrophila* challenge. C: Heatmap showing expression of representative genes in each conserved IgM⁺ B cell subpopulation before and after *A. hydrophila* challenge. GenBank accession numbers are as follows: thioredoxin- interacting protein (*TXNIP*: XM_051871792.1), DNA damage-inducible transcript 4 (*DDIT4*: XM_051915381.1), sestrin-1 (*SESN1*: XM_051874404.1) transcription factor Jun-B (*JunB*: DQ298415.1), growth arrest and DNA-damage-inducible beta (*GADD45B*: MH046777.1), Krüppel-like factor 2 (*KLF2*: XM_051910529.1), forkhead box O3B (*FOXO3*: XM_051874162.1), induced myeloid leukemia cell differentiation protein Mcl-1 homolog (*MCL1*: XM_051866610.1), B-cell linker protein-like (*BLNK*: XM_051916847.1), cluster of differentiation 79b (*CD79b*: XM_051915348.1), natural killer-enhancing factor B (*NKEFB*: JX021298.1), class of major histocompatibility complex Ⅱ β (*MHC Ⅱβ*: XM_051904050.1). Avg.exp represents normalized average expression value of a gene within cell subpopulations. D: Violin plots showing phagocytosis, antigen processing, and presentation scores for each conserved IgM⁺ B cell subpopulation. ns: Not significant; *: $P<0.05$; **: $P<0.01$;

***: $P<0.001$; ****: $P<0.0001$. E: Monocle trajectories of conserved IgM⁺ B cell subpopulations. Each dot represents a single cell. F: Velocity analysis showing inter-relationship of IgM⁺ B cell subpopulations. Velocity fields were projected onto the UMAP plot. Left side represents control group and right side represents infection group.

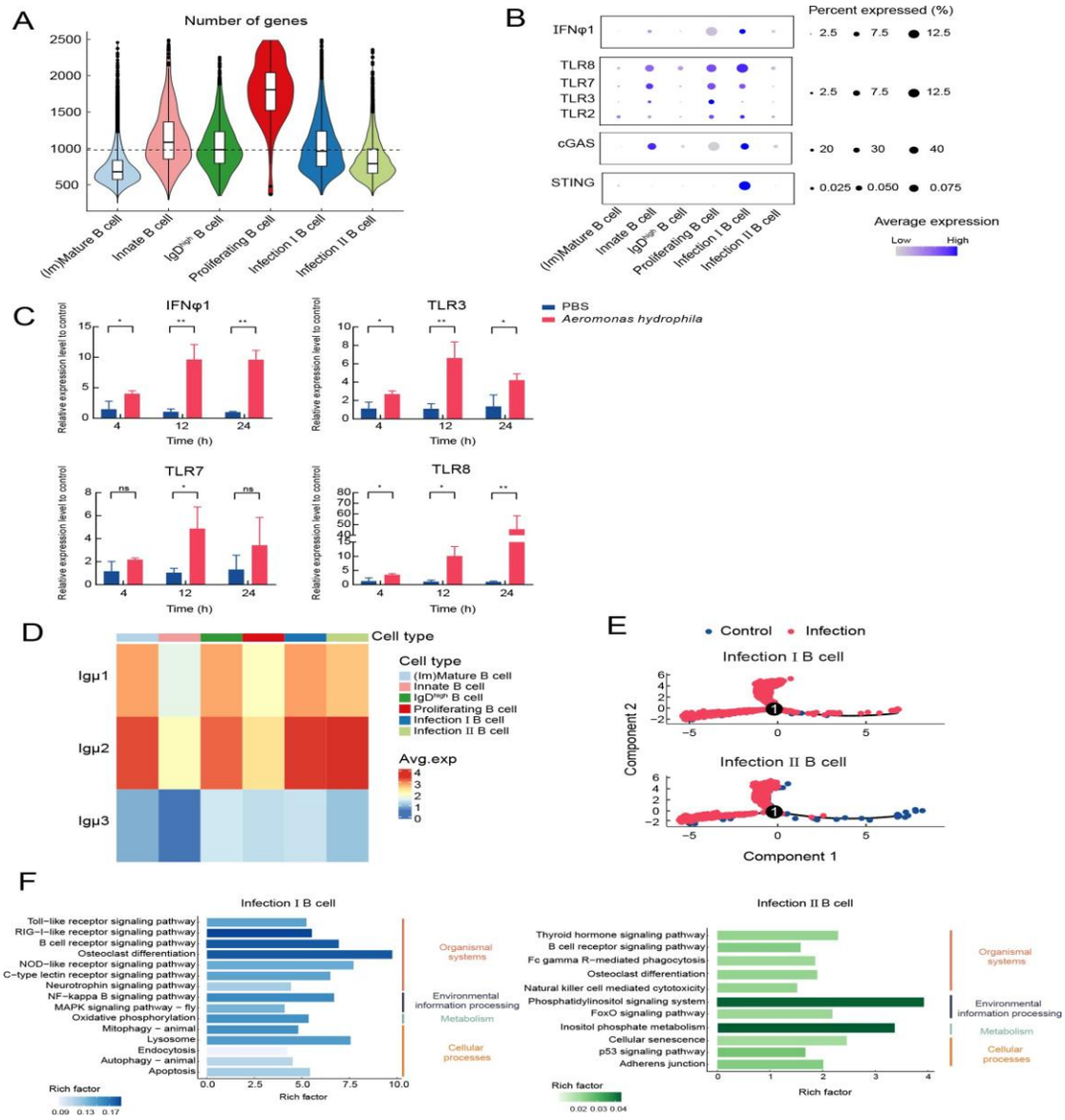

Figure 5 Characterization of newly emerged peripheral blood IgM⁺ B cell subpopulations following bacterial infection

A: Violin plots showing number of genes expressed in peripheral blood IgM⁺ B cell subpopulations from infected grass carp. B: Dot plot showing expression of IFN-related genes in peripheral blood IgM⁺ B cell subpopulations from infected grass carp. GenBank accession numbers are as follows: interferon φ1 (*IFNφ1*: AB180663.1), toll-like receptor 2 (*TLR2*: XM_051918532.1), toll-like receptor 3 (*TLR3*: XM_051893528.1), toll-like receptor 7 (*TLR7*: XM_051904961.1), toll-like receptor 8 (*TLR8*: XM_051904962.1), cyclic GMP-AMP synthase (*cGAS*: XM_051915779.1), stimulator of interferon gene (*STING*: KF494194.1). C: Relative expression of IFN-related genes in peripheral blood IgM⁺ B cells after *A. hydrophila* stimulation (n=3). Expression (fold change) of IFN-related genes after *A. hydrophila* stimulation was calculated by comparing stimulated cells with control cells using the $2^{-\triangle\triangle Ct}$ method. Data are mean±SD. ns: Not significant; *: P<0.05; **: P<0.01. D: Heatmap showing expression of *Igμ* subclasses in IgM⁺ B cell subpopulations after *A. hydrophila* challenge. Avg.exp represents normalized average expression value of a gene within cell subpopulations. E: Monocle trajectories of infection Ⅰ and Ⅱ B cells. Each dot represents a single cell. F: KEGG enrichment analysis of DEGs in infection Ⅰ (left) and Ⅱ B cell (right) subpopulations that emerged following infection.

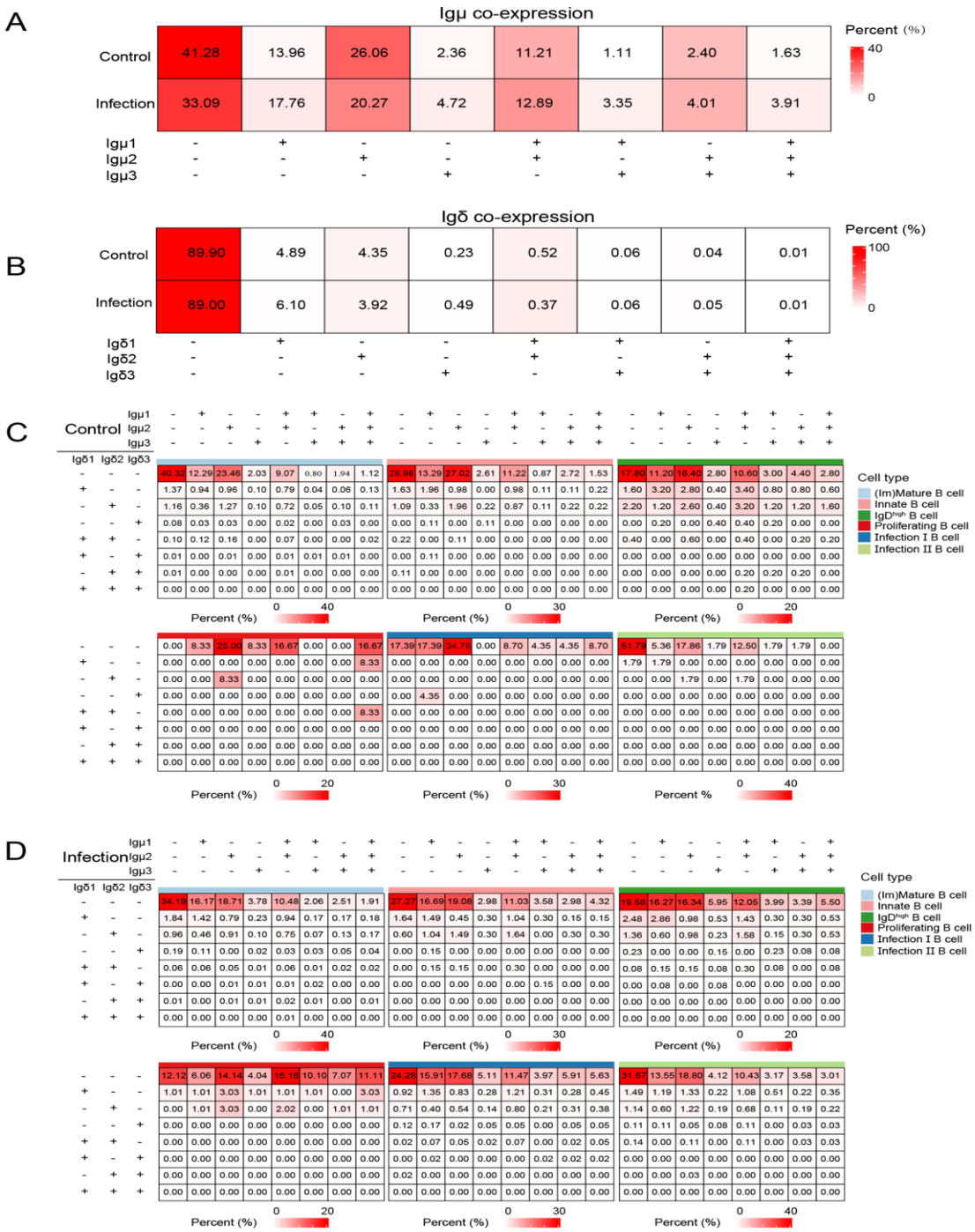

Figure 6 Co-expression of immunoglobulin subclass genes in grass carp peripheral blood IgM⁺ B cells

A: Heatmap showing percentage of peripheral blood IgM⁺ B cells expressing *Igμs*. B: Heatmap showing percentage of peripheral blood IgM⁺ B cells expressing *Igδs*. C: Heatmap showing expression patterns of *Igμs* and *Igδs* in peripheral blood IgM⁺ B cells from control grass carp. D: Heatmap showing expression patterns of *Igμs* and *Igδs* in peripheral blood IgM⁺ B cells from infected grass carp. +, positive; −, negative.

cells, CD22$^+$ cells, and CD34$^+$ cells (Pan et al., 2023). To further explore the heterogeneity of peripheral IgM$^+$ B cells and their response to bacterial infection, scRNA-seq was applied to sorted populations from grass carp. Results revealed six major IgM$^+$ B cell subpopulations, including (im)mature, innate, proliferating, IgD^{high}, infection Ⅰ, and infection Ⅱ B cells. Among them, IgD^{high}, infection Ⅰ, and infection Ⅱ B cells were not detected in the head kidney (Pan et al., 2023), indicating compartment-specific divergence of B cell states. These findings suggest that peripheral B cells in teleosts, as in mammals, exhibit microenvironmental heterogeneity and functional diversity, including antibody secretion, cytokine production, and phagocytosis (Abós et al., 2015; Han et al., 2024).

IgD displays significant structural and functional plasticity across vertebrate lineages, largely attributable to variation in the number and composition of Cδ domains (Sun et al., 2020). In teleosts, IgD exhibits greater complexity due to frequent duplication and deletion events involving specific *Cδ* exons. This genomic plasticity has resulted in the emergence of multiple IgD subclasses in species such as channel catfish (*Ictalurus punctatus*), medaka (*Oryzias latipes*), and Atlantic salmon (*Salmo salar*) (Bengtén et al., 2002; Hordvik, 2002; Magadán-Mompó et al., 2011). In mammals, surface expression of IgD-B cell receptor (BCR) is absent on immature B cells, low on transitional B cells, and highest on mature follicular B cells (Avrameas et al., 1979). Similarly, most teleost B cells co-express surface IgM and IgD, with IgD expression typically down-regulated following antigen engagement, reflecting a conserved activation trajectory similar to the behavior of mammalian B cells (Tafalla et al., 2017). We previously identified three *Igδ* genes in the grass carp genome, each encoding different numbers of *Cδ2-Cδ3- Cδ4* domain repeats (Pan et al., 2023). In the current study, three Ig*δ* genes were highly expressed in a distinct IgM$^+$ B cell subpopulation termed IgD^{high} B cells. This subpopulation demonstrated transcriptional enrichment in phagocytosis-related pathways and protein-related genes associated with translation and peptide biosynthesis. IgD^{high} B cells displayed higher *Igμs* expression than (im)mature B cells and a proliferative index second only to proliferating B cells, supporting their classification as mature B cells and suggesting that IgD is preferentially expressed at this stage. Previous studies have reported that peripheral IgM$^+$IgD$^+$ B cells in rainbow trout may represent a mature B cell subset with high antigen-presenting capacity (Perdiguero et al., 2021). Similarly, grass carp IgD^{high} B cells were also enriched in the MHC class Ⅱ protein complex pathway, suggesting a conserved immunological role across teleost species. Notably, a small proportion of plasma cells (Irf4$^+$IgM^{high}IgD^{low}) have been found in the peripheral blood of rainbow trout, comprising only 0.40% of circulating B cells (Perdiguero et al., 2024). In contrast, no transcriptionally defined plasma cell subpopulation was identified in the peripheral IgM$^+$ B cell compartment of grass carp in this study, suggesting that peripheral blood is not a major reservoir for plasma cells in teleosts.

Extensive crosstalk between metabolic reprogramming and B cell fate underscores the importance of nutrient availability and utilization in shaping B cell immune responses (Fu et al., 2022; Jellusova, 2020). Although BCR engagement enhances cellular glucose uptake and glycolytic flux, certain B cell subsets, such as murine germinal center B cells, preferentiallyrely on fatty acid oxidation for energy (Chen et al., 2021; Weisel et al., 2020). Despite the absence of germinal center- like structures in peripheral blood, grass carp IgD^{high} B cells preferentially utilized fatty acid metabolism relative to other subpopulations. Elevated OXPHOS activity in proliferating B cells suggests a metabolic reliance on the pentose phosphate pathway rather than glycolysis or fatty acid oxidation, consistent with demands for nucleotide biosynthesis and redox regulation (Teslaa et al., 2023). Pathogen-induced metabolic stress is known to drive B cell transformation, as exemplified by Epstein-Barr virus targeting the mitochondrial 1C pathway to support rapid B cell expansion (Rodda & Pepper,

2020; Wang et al., 2019). In the present study, *A. hydrophila* infection markedly increased energy demands in grass carp IgM^+ B cells, accompanied by enhanced fatty acid metabolism and up-regulation of *SNAT2* (*SLC38A2*) in specific subpopulations, highlighting fatty acids and amino acids as key metabolic substrates for antibacterial defense. These findings suggest that dietary supplementation with fatty acids and amino acids may augment teleost B-cell mediated anti- infective activity.

In mammals, certain B cell subpopulations contribute to immunoregulation by secreting cytokines; for instance, regulatory B cells secrete anti-inflammatory mediators such as IL-10, IL-35, and transforming growth factor (TGF)-β to suppress inflammation (Rosser & Mauri, 2015). In contrast, cytokine-producing B cell populations in teleosts remain poorly characterized. Notably, this study identified a distinct IgM^+ B cell subpopulation in grass carp peripheral blood that expressed *IFNφ1* following bacterial challenge. While type I IFNs (IFN-I) have garnered considerable attention due to their protective role in antiviral immunity, recent studies have demonstrated that they also play a crucial role in host antibacterial immunity (González-Navajas et al., 2012; Monroe et al., 2010). Teleosts possess a diverse repertoire of IFN-I genes, with grass carp encoding four IFN-I isoforms (*IFNφ1–4*), orthologous to those in zebrafish (Liao et al., 2016). Among them, IFNφ1 has demonstrated broad- spectrum bactericidal activity (Xiao et al., 2021; Zhu et al., 2023). The *IFN-I* expressed by the newly identified subpopulation was confirmed to be *IFNφ1*. Similarly, pathogen stimulation in mice leads to the emergence of non-canonical B cell subsets with atypical immune functions, including the production of high levels of IFN-γ, which enhances macrophage activation and initiates innate immune responses (Bao et al., 2014). These findings indicate that the ability of B cells to secrete IFNs in response to infection is evolutionarily conserved from teleosts to mammals, although the specific IFN types produced differ among lineages.

This study provides a comprehensive single-cell characterization of peripheral blood IgM^+ B cells in grass carp, revealing substantial heterogeneity in their molecular profiles. Upon bacterial infection, specific IgM^+ B cell subpopulations exhibited activation and underwent distinct metabolic reprogramming. Notably, a previously uncharacterized subpopulation capable of secreting IFNφ1 was induced in response to infection. These findings suggest that bacterial vaccination may simultaneously activate both antibody production and IFNφ1-mediated immune responses in teleosts, potentially conferring broad-spectrum immune protection against bacterial and viral pathogens. Validation of this hypothesis will contribute to the development of next- generation vaccines in aquaculture. Collectively, these

findings provide novel insights into the mechanisms by which circulating IgM^+ B cells defend against bacterial infections in teleost fish.

DATA AVAILABILITY

The single-cell sequencing data generated in this study have been deposited in the Genome Sequence Archive (GSA) (https://www.scidb.cn/en/c/zoores) under CRA023998, Science Data Bank (doi: 10.57760/ sciencedb.j00139.00185), and NCBI (https://www.ncbi.nlm.nih.gov/) under BioProjectID PRJNA1010877.

SUPPLEMENTARY DATA

Supplementary data to this article can be found online.

COMPETING INTERESTS

The authors declare that they have no competing interests.

AUTHORS' CONTRIBUTIONS

Experimental design and conception: X.J.Z., Y.A.Z.; investigation: Y.R.P., X.Q.H., T.T.T.; formal analysis: Y.R.P.; writing-original draft: Y.R.P.; writing- review & editing: X.J.Z., Y.A.Z.; experimental organization and analysis supervision: X.J.Z., Y.A.Z. All authors read and approved the final version of the manuscript.

ACKNOWLEDGMENTS

We thank Yan Wang (Analysis and Testing Center, Institute of Hydrobiology, Chinese Academy of Sciences) for technical assistance in cell sorting.

REFERENCES

Abós B, Castro R, Granja AG, et al. 2015. Early activation of teleost B cells in response to rhabdovirus infection. *Journal of Virology*, **89**(3): 1768–1780. Akkaya M, Kwak K, Pierce SK. 2020. B cell memory: building two walls of protection against pathogens. *Nature Reviews Immunology*, **20**(4): 229–238.

Amemiya CT, Alföldi J, Lee AP, et al. 2013. The African coelacanth genome provides insights into tetrapod evolution. *Nature*, **496**(7445): 311–316.

Avrameas S, Hösli P, Stanislawski M, et al. 1979. A quantitative study at the single cell level of immunoglobulin antigenic determinants present on the surface of murine B and T lymphocytes. *The Journal of Immunology*, **122**(2): 648–659.

Baik SY, Yun HS, Lee HJ, et al. 2007. Identification of stathmin 1 expression induced by Epstein-Barr virus in human B lymphocytes. *Cell Proliferation*, **40**(2): 268–281.

Bantug GR, Galluzzi L, Kroemer G, et al. 2018. The spectrum of T cell metabolism in health and disease. *Nature Reviews Immunology*, **18**(1): 19–34.

Bao Y, Liu XG, Han CF, et al. 2014. Identification of IFN-γ-producing innate B cells. *Cell Research*, **24**(2): 161–176.

Bénard A, Sakwa I, Schierloh P, et al. 2018. B cells producing type I IFN modulate macrophage polarization in tuberculosis. *American Journal of Respiratory and Critical Care Medicine*, **197**(6): 801–813.

Bengtén E, Quiniou SMA, Stuge TB, et al. 2002. The *IgH* locus of the channel catfish, *Ictalurus punctatus*, contains multiple constant region gene sequences: different genes encode heavy chains of membrane and secreted IgD. *The Journal of Immunology*, **169**(5): 2488–2497.

Bergen V, Lange M, Peidli S, et al. 2020. Generalizing RNA velocity to transient cell states through dynamical modeling. *Nature Biotechnology*, **38**(12): 1408–1414.

Bhattacharya M. 2018. Understanding B lymphocyte development: a long way to go. In: Istifli ES, İla HB. Lymphocytes. IntechOpen.

Cancro MP. 2020. Age-associated B cells.

Annual Review of Immunology, **38**(1): 315–340.

Castro R, Abós B, González L, et al. 2015. Molecular characterization of CD9 and CD63, two tetraspanin family members expressed in trout Blymphocytes. *Developmental & Comparative Immunology*, **51**(1): 116–125.

Chen CF, Laidlaw BJ. 2022. Chapter one - development and function of tissue-resident memory B cells. *Advances in Immunology*, **155**: 1–38.

Chen DY, Wang Y, Manakkat Vijay GK, et al. 2021. Coupled analysis of transcriptome and BCR mutations reveals role of OXPHOS in affinity maturation. *Nature Immunology*, **22**(7): 904–913.

Cui ZW, Zhang XY, Wu CS, et al. 2020. Membrane IgM^+ plasma cells in grass carp (*Ctenopharyngodon idella*): insights into the conserved evolution of IgM^+ plasma cells in vertebrates. *Developmental & Comparative Immunology*, **106**: 103613.

Dabiri GA, Young CL, Rosenbloom J, et al. 1992. Molecular cloning of human macrophage capping protein cDNA. A unique member of the gelsolin/villin family expressed primarily in macrophages. *Journal of Biological Chemistry*, **267**(23): 16545–16552.

De Gruijter NM, Jebson B, Rosser EC. 2022. Cytokine production by human B cells: role in health and autoimmune disease. *Clinical and Experimental Immunology*, **210**(3): 253–262.

Erttmann SF, Swacha P, Aung KM, et al. 2022. The gut microbiota prime systemic antiviral immunity via the cGAS-STING-IFN-I axis. *Immunity*, **55**(5): 847–861. e10.

Ferrero G, Gomez E, Lyer S, et al. 2020. The macrophage-expressed gene (*mpeg*) 1 identifies a subpopulation of B cells in the adult zebrafish. *Journal of Leukocyte Biology*, **107**(3): 431–443.

Fooksman DR, Jing ZX, Park R. 2024. New insights into the ontogeny, diversity, maturation and survival of long-lived plasma cells. *Nature Reviews Immunology*, **24**(7): 461–470.

Frasca D, Diaz A, Romero M, et al. 2019. Metabolic requirements of human pro-inflammatory B cells in aging and obesity. *PLoS One*, **14**(7): e0219545. Fu Y, Wang LM, Yu BC, et al. 2022. Immunometabolism shapes B cell fate and functions. *Immunology*, **166**(4): 444–457.

García-Vega M, Llamas-Covarrubias MA, Loza M, et al. 2024. Single-cell transcriptomic analysis of B cells reveals new insights into atypical memory B cells in COVID-19. *Journal of Medical Virology*, **96**(8): e29851.

González-Navajas JM, Lee J, David M, et al. 2012. Immunomodulatory functions of type I interferons. *Nature Reviews Immunology*, **12**(2): 125–135.

Guslund NC, Solbakken MH, Brieuc MSO, et al. 2020. Single-cell transcriptome profiling of immune cell repertoire of the Atlantic cod which naturally lacks the major histocompatibility class II system. *Frontiers in Immunology*, **11**: 559555.

Han XQ, Cui ZW, Ma ZY, et al. 2024. Phagocytic plasma cells in teleost fish provide insights into the origin and evolution of B cells in vertebrates. *The Journal of Immunology*, **213**(5): 730–742.

Hao Y, O'Neill P, Naradikian MS, et al. 2011. A B-cell subset uniquely responsive to innate stimuli accumulates in aged mice. *Blood*, **118**(5): 1294–1304.

Hart GT, Wang XD, Hogquist KA, et al. 2011. Krüppel-like factor 2 (KLF2) regulates B-cell reactivity, subset differentiation, and trafficking molecule expression. *Proceedings of the National Academy of Sciences of the United*

States of America, **108**(2): 716–721.

Hinman RM, Nichols WA, Diaz TM, et al. 2009. *Foxo3*-/- mice demonstrate reduced numbers of pre-B and recirculating B cells but normal splenic B cell sub-population distribution. *International Immunology*, **21**(7): 831–842.

Hoffman W, Lakkis FG, Chalasani G. 2016. B cells, antibodies, and more. *Clinical Journal of the American Society of Nephrology*, **11**(1): 137–154. Hordvik I. 2002. Identification of a novel immunoglobulin δ transcript and comparative analysis of the genes encoding IgD in Atlantic salmon and Atlantic halibut. *Molecular Immunology*, **39**(1-2): 85–91.

Hu CB, Zhang N, Hong Y, et al. 2024. Single-cell RNA sequencing unveils the hidden powers of zebrafish kidney for generating both hematopoiesis and adaptive antiviral immunity. *eLife*, **13**: RP92424.

Jellusova J. 2020. Metabolic control of B cell immune responses. *Current Opinion in Immunology*, **63**: 21–28.

Kaminski DA, Wei CW, Qian Y, et al. 2012. Advances in human B cell phenotypic analysis. Immunological Frontiers, 3: 302.

Fan J, Millard N, Korsunsky I, et al. 2019. Harmony's single-cell data integration is quick, sensitive, and precise. 1289–1296 in Nature Methods, 16(12).

La Soldatov R, Zeisel A, Manno G, et al. 2018. single-cell RNA velocity. 494–498 in Nature, 560(7719).

Lebien TW, Tedder TF. 2008. The development and function of B cells. 112(5): 1570–1580; Blood.

Wan QY, Liao ZW, and Su JG. 2016. The grass carp Ctenopharyngodon idella's IFNs, IRFs, and CRFBs were characterized organizationally and expressionally using bioinformatics. Comparative & Developmental Immunology, 61: 97–106.

Alpuche-Aranda C, Perez-Lopez A, Lopez-Medina M, et al. 2015. Salmonella causes B cells to express PD-L1. Letters on Immunology, 167(2): 131–140.

Lund FE. 2008. B lymphocytes that produce cytokines are important immune regulators. Immunology: Current Opinion, 20(3): 332–338.

Tedder TF, Candando KM, and Lykken JM. 2015. regulate the growth and operation of B10 cells. 471–477 in International Immunology, 27(10).

Magnoglobulin heavy chains in medaka (Oryzias latipes) were examined by Magadán-Mompó S, Sánchez-Espinel C, and Gambón-Deza F. (2011). 11(1): 165 in BMC Evolutionary Biology.

Gohar A, van Duijvenvoorde A, Meeuwsen JAL, et al. 2017. In individuals with advanced atherosclerotic disease, higher levels of (un)switched memory B lymphocytes are linked to better outcomes. American Heart Association Journal, 6(9): e005747.

Vance RE, McWhirter SM, and Monroe KM. 2010. bacterial induction of type I interferons. Microbiology of Cells, 12(7): 881–890.

Tergaonkar V, Morgan D. 2022. B cell trajectories are unraveled at the single cell level. 210–229 in Trends in Immunology, 43(3).

Letai A, Beard C, Opferman JT, et al. (2003). Antiapoptotic MCL-1 is necessary for the development and maintenance of B and T cells. Nature, 426(6967): 671–676.

Wu CS, Zhong YQ, Pan YR, et al. 2023. The distinct variety of B cells in early vertebrates is revealed by an atlas of grass carp IgM+ B cells in homeostasis and bacterial infection. 964–980 in The Journal of Immunology, 211(6).

Kehry MR, Pearson LL, and Castle BE. 2001. Tumor necrosis factor receptor-associated factor mRNAs are up-regulated and mitogen-activated protein kinase signaling pathways are activated in monocytic cells through CD40-mediated signaling. 13(3): 273–283 in International Immunology.

Jiménez-Barrios P, Morel E, Perdiguero P, et al. 2024. Peripheral blood leukocyte single-cell atlas of rainbow trout and early response profile to infectious pancreatic necrosis virus. Immunological Frontiers, 15: 1404209.

Tafalla C., Morel E., and Perdiguero P. 2021. Single-cell RNA sequencing demonstrated the diversity of rainbow trout blood B cells. 10(6), Biology, 511.

Chen SY, Peuß R, Box AC, et al. 2020. Cavefish immune investment and immunopathological

responses are impacted by adaptation to reduced parasite prevalence. Ecology & Evolution in Nature, 4(10): 1416–1430.
Tang Y, Qiu XJ, Mao Q, et al. 2017. Complex single-cell trajectories can be resolved via reversed graph embedding. 979–982 in Nature Methods, 14(10).
Boboila C, Corbett E, Repasky JAE, et al. 2004. Mutational investigation of N-nucleotide addition in V(D)J recombination mediated by terminal deoxynucleotidyltransferase. 5478–5488 in The Journal of Immunology, 172(9).
Pepper M, Rodda LB. 2020. metabolic limitations on the malaria response of B cells. 722–724 in Nature Immunology, 21(7).
Mauri C., Rosser EC. 2015. Origin, characteristics, and role of regulatory B cells. 42(4), Immunity, 607–612.
Wei CW, Lee FEH, Sanz I, et al. (2008). Variability in human memory B cell phenotype and function. Immunology Seminars, 20(1): 67–82.
Gennert D, Satija R, Farrell JA, et al. (2015). reconstruction of single-cell gene expression data in space. 33(5), Nature Biotechnology, 495–502.
Shin D, Shao Y, Kim SY, et al. (2010). By inhibiting the expression of BCL-6, TXNIP controls the formation of germinal centers. 78–84 in Immunology Letters, 129(2).
Fillatreau S. and Shen P. (2015). B cells' antibody-independent roles: an emphasis on cytokines. Immunology in Nature Reviews, 15(7): 441–451.
Shibasaki Y, Fernández-Montero A, Afanasyev S, et al. 2023. Organized structures resembling germinal centers originated in cold-blooded vertebrates. eadf1627 in Science Immunology, 8(90).
Kardava L, Silva R, Moir S, et al. 2011. Human B cells contain CD300a, which controls BCR-mediated signaling and has down-regulated expression in HIV infection. 117(22): 5870–5880; Blood.
Su JG. 2025. Teleosts' toll-like receptor signaling. doi: https://doi.org/10.1007/s11427-024-2822-5, Science China Life Sciences.
In 2020, Sun Y, Huang T, Hammarström L, et al. New perspectives, ramifications, and uses for immunoglobulins. 145–169 in Annual Review of Animal Biosciences, 8(1).
Castro R, Tafalla C, González L, et al. (2017). A subset of teleost fish's splenic B cells release B cell-activating factor, which controls several aspects of B cell function. Immunology Frontiers, 8: 295.
Terada N, Lucas JJ, Takase K, et al. 1995. regulation of human B lymphocytes activated by mitogens in terms of cell cycle entry and progression. Cellular Physiology Journal, 162(2): 246–255.
Iyer S, Lobbardi R, Tang Q, et al. 2017. RNA sequencing is used to analyze the heterogeneity of hematopoietic and renal cells in adult zebrafish at the single-cell level. Experimental Medicine Journal, 214(10): 2875–2887.
Fan J, Ralser M, Teslaa T, et al. 2023. In both health and illness, the pentose phosphate pathway is involved. 1275–1289 in Nature Metabolism, 5(8).
Van Spriel AB, Van Der Schaaf A, De Keijzer S, et al. (2012). The tetraspanin CD37 promotes long-term plasma cell survival by coordinating the α4β1 integrin-Akt signaling axis. ra82 in Science Signaling, 5(250).
Shen HY, Nobre L, Wang LW, et al. 2019. B cell metamorphosis is driven by one-carbon metabolism mediated by the Epstein-Barr virus. 30(3): 539–555. e11. Cell Metabolism.
Mullett SJ, Elsner RA, Weisel FJ, et al. 2020. While performing little glycolysis, germinal center B cells specifically oxidize fatty acids for energy. 331–342 in Nature Immunology, 21(3).
Jansen K, Wirz OF, Satitsuksanoa P, et al. 2022. Patients with asthma experience dysregulation of the antiviral response that is induced in circulating B lymphocytes by experimental rhinovirus infection. 77(1): 130–142; Allergy.
Wu CS, Zheng GD, Ma ZY, et al. 2022. The grass carp's (Ctenopharyngodon idella) chromosome-level genome assembly sheds light on the evolution of its genome. BMC Genomics, 23(1), 271.
Li L, Wu LT, Gao AL, et al. (2021). Anterior kidney leukocytes from nile tilapia (Oreochromis niloticus) were profiled using a single-cell transcriptome. Immunology Frontiers, 12: 783196.
Zhang YQ, Zhu WT, Xiao X, and others (2021). The antimicrobial peptide-like action of type I IFNs in vertebrates is revealed by the broad-

spectrum strong direct bactericidal activity of fish IFNφ1. 1337–1347 in The Journal of Immunology, 206(6).

Li J, Salinas I, Zhang YA, et al. (2010). Mucosal immunity is the focus of the primitive immunoglobulin class IgT. 827–835, Nature Immunology, 11(9).

Liao Z, Zhang Y, Zhu W, et al. 2023. IFN1 promotes antibacterial immune modulation in teleosts and increases thrombocyte phagocytosis via the IFN receptor complex-JAK/STAT-complement C3.3-CR1 pathway. Immunology Journal, 210(8): 1043–1058.

Zwollo P. (2011). using transcription factors to analyze the differentiation of teleost B cells. Immunology in Development and Comparison, 35(9): 898–905.